

2. Fisher Forecast Formalism

$$T_{\text{obs}} = \bar{T}(1 + \delta T)$$

而在某 voxel 中的 δT 可以分为

$$\delta T = \delta T^{\text{signal}}(\vec{\theta}_p, \nu_p) + \delta T^{\text{noise}}(\vec{\theta}_p, \nu_p) + \delta T^{\text{foreground}}(\vec{\theta}_p, \nu_p)$$

在 voxel 和 comoving-space location 之间的映射为

$$\begin{cases} \vec{\nu}_L = \nu(z_i) [\vec{\theta}_p - \vec{\theta}_i] \\ \vec{\nu}_{\parallel} = \frac{c(z_i)}{H(z_i)} (\vec{\nu}_p - \vec{\nu}_i) = \gamma_{\nu}(z_i) (\vec{\nu}_p - \vec{\nu}_i) \end{cases}$$

其中, $\gamma(z) = \int_0^z \frac{cdz}{H(z)}$ ($\Omega_k = 0$), $\gamma_{\nu} = \frac{d\nu}{dz} dz$

$\rightarrow \gamma(z)$ 共动距离半径 \Rightarrow 定义为光走过的距离

$\tilde{\omega}$ 称为 dimensionless frequency, $\tilde{\omega} = \frac{1}{1+z} = \frac{\nu}{\nu_{\text{obs}}}$

定义以上坐标后, 可以写入 FT. (3 dim)

$$\delta T(\vec{q}, \nu) = \int \delta T(\vec{\theta}, \nu) e^{i(\vec{\theta} \cdot \vec{q} + \nu \cdot \tilde{\omega})} d^2\theta d\nu$$

不用考虑元素的协方差, 可以使用

$$\langle \delta T^{x*}(\vec{q}, \nu) \delta T^x(\vec{q}', \nu') \rangle = (2\pi)^3 C^x(\vec{q}, \nu) \delta^2(\vec{q} - \vec{q}') \delta(\nu - \nu') \delta(x)$$

\Rightarrow 近似: ① signal, foreground, noise 互不相关

(不严密, 由于去除前景的过程会引入相关性)

(只有在 flat-sky 近似下 signal 才和其他两者不相关)

(Galaxy foreground 是各向异性的)

② 忽略 redshift bin 内部的演化 \Rightarrow 粒点化

2.1 对 signal 建模

$$T_b = \frac{c^2 I_b}{2 k_B T^2} = \bar{T}_b (1 + \delta_{HI})$$

而：

$$\bar{T}_b = \frac{3}{32\pi} \frac{\hbar c^3 A_{10}}{k_B m_p v_{1cm}^2} \frac{(1+z)^2}{H(z)} \Omega_{HI}(z) \rho_{m0}$$

所以 $\delta T^s(\vec{q}_p, v_p) = \bar{T}_b(z) \delta_{HI}(\vec{r}_p, z)$

* HI 多处于星系内的相同密度团内，所以可作为星系示踪。

$$\delta_{HI} = b_{HI} * \delta_m, * = convolution$$

变换后和 δ_{HI} 可写成：

$$\delta_{HI}(\vec{k}) = (b_{HI} + f\mu^2) e^{-\frac{k^2 \sigma_m^2}{2}} \delta_m(\vec{k}), \mu = \frac{k_m}{k}$$

线性增长因子 小尺度上不相关的速度项到起始上帝之指效应。

这是由于 HI intensity 变为 $I(v)$ ，则要考虑 redshift space distortion

角量影响

利用各向同性物质功率谱的定义，可以得到：

$$\langle \delta_m^*(\vec{k}) \delta_m(\vec{k}) \rangle = (2\pi)^3 P(k) \delta^3(\vec{k} - \vec{k}')$$

联立可以得到：

$$\begin{aligned} \langle \delta T^s(\vec{q}, y) \delta T^s(\vec{q}', y') \rangle &= \bar{T}_b^2(z) \langle \delta_{HI}^* \delta_{HI} \rangle \\ &= \bar{T}_b^2(z) (b_{HI} + f\mu^2)^2 \exp(-k^2 \mu^2 \sigma_m^2) (2\pi)^3 P(k) \delta^3(\vec{k} - \vec{k}') \end{aligned}$$

$$= (2\pi)^3 C^s(\vec{q}, y) \delta^3(\vec{q} - \vec{q}') \delta(y - y') \delta_{SS} \quad ?$$

可以得到： $\delta^2(\vec{q} - \vec{q}') = \delta^2(r(\vec{k}_\perp - \vec{k}'_\perp))$

$$= r^2 \delta^2(\vec{k}_\perp - \vec{k}'_\perp)$$

$$\begin{cases} \int \delta(x) dx = 1 \\ \int \delta(kx) dk = 1 \\ \frac{1}{k} \int \delta(kx) dk = \delta(x) \end{cases}$$

即：

$$\nu^2 \nu_\nu C^S(\vec{q}, y) = T_b(z) (b_{\text{HI}} + f \mu^2) \exp(-k^2 \mu^2 \sigma_{\text{NL}}^2) P(k)$$

$$C^S(\vec{q}, y) = \frac{T_b^2(z)}{\nu^2 \nu_\nu} (b_{\text{HI}} + f \mu^2) \exp(-k^2 \mu^2 \sigma_{\text{NL}}^2) [P(k, z=0) D(z)]$$

线性增长因子

growth rate:

$$f = \frac{d \ln D}{d a}$$

$$= \Omega_m(z)$$

$$\Omega_m(z) = \Omega_m(1+z)^3 \frac{H_0^2}{H(z)^2}$$

不随红移变化的源：

① b_{HI} \Rightarrow 和 host dark matter halo 有关

依赖性可表达为“有大团的低质量截断”

halo mass function.

② HI density function $\Omega_{\text{HI}} = \frac{\rho_{\text{HI}}}{\rho_{c,0}}$



best constraints on HI fraction: (Switzer et al. 2013)

$$S_{\text{HI}} b_{\text{HI}} = (4.3 \pm 1.1) \times 10^{-4} \text{ at } 68\% \text{ confidence level, } z=0.8$$

③ $\sigma_{\text{NL}} \sim 4 \sim 10 \text{ Mpc}$

2.2. noise 和 beam 的模型

\Rightarrow 噪声协方差模型

$$C^N(\vec{q}, y) = \frac{T_{\text{sys}}^2}{t_{\text{int}} \Delta \tilde{\nu}} U_{\text{bin}} L B_{\perp}^{-2} B_{\parallel}^{-1}$$

T_{sys} : 系统温度

$$U_{\text{bin}} = S_{\text{area}} \Delta \tilde{\nu} \quad S_{\text{area}}: \text{Survey area}$$

$\Delta \tilde{\nu}$: dimensionless bandwidth within the velocity bin

L, B : 描述 receiver 的类型 / 数密度 和其对角度和步进率
的相关性。

⇒ 系统温度的两个分量.

$$T_{\text{sys}} = \begin{cases} T_{\text{inst}}: \text{和硬件有关} \\ T_{\text{sky}} \sim 60K \times \left(\frac{\nu}{300 \text{MHz}} \right)^{-2.5} \text{ 大气辐射等背景辐射.} \end{cases}$$

⇒ effective beam term.

径向分辨率和带宽 $\Delta\nu$ 有关

$$B_{\perp}(y) = \exp\left(-\frac{(y\Delta\nu/\nu_{\text{Lc.m}})^2}{16\ln 2}\right)$$

↑
系数和 FWHM (半峰宽度)
的定义有关.

$$\sigma = \Theta_{\text{FWHM}} \sqrt{8\ln 2}$$

⇒ L : dish multiplicity factor

B_{\perp} : transverse effective beam.

和是 SD 还是 IF 有关.

$$L = \frac{f(\nu)}{N_b N_d} \quad B_{\perp}(\vec{q}) = \exp\left(-\frac{(2\Theta_b)^2}{16\ln 2}\right)$$

其中. $\Theta_b = \lambda/D_{\text{dish}}$. 单一 dish 的 FWHM

N_d : dish 的数量.

N_b : beam 的数量

$f(\nu)$: 不同波长的频率依赖

⇒ 对于 IF, 有

$$LB_{\perp}^{-2} = \frac{FOV}{n(u=9/2\pi)} \quad n(u) \text{ number density of samples in } uv \text{ plane}$$

$$FOV \sim \left(\frac{\lambda}{D_{\text{dish}}}\right)^2 \text{ 视场}$$

其中进一步有

$$n(\nu) = \frac{N\alpha(\alpha-1)}{2\pi(U_{\max}^2 - U_{\min}^2)}$$

$$U_{\max} = D_{\max}/\lambda, U_{\min} = D_{\min}/\lambda$$

D_{\max}/λ 分别为最长/最短的基线

2.3 Foreground 的模型

前景来源: galaxy, extragalactic point source.

Belief: 已经通过某些方法消除了前景, 但是有残留污染, 其 variance 可以建模为平滑功率谱

residual foreground 的模型为

$$C_F(\vec{q}, p) = C_{Fq} \sum_X A_X \left(\frac{\ell_p}{2\pi q} \right)^{n_X} \left(\frac{D_p}{D_i} \right)^{m_X}$$

对于不同前景(X) 的方差如下

不是很明白

Foreground	$A_X [\text{mK}^2]$	n_X	m_X
Extragalactic point sources	57.0	1.1	2.07
Extragalactic free-free	0.014	1.0	2.10
Galactic synchrotron	700	2.4	2.80
Galactic free-free	0.088	3.0	2.15

$$(\ell_p = 1000, D_p = 130 \mu\text{m}^{-1})$$

C_{Fq} 表达前景移除的效率。

$C_{Fq}=1$ 对应本源前景。

一般 $C_{Fq} \sim 10^{-5}$

(与上泡的) 前景合成与之间的
关联)

2.4. Fisher Matrix.

建立渐近统计用的 Fisher 矩阵.

⇒ 将 \vec{y} 和 \vec{q} 的所有独立的模求和.

$$\Delta y = \frac{2\pi}{\Delta \vec{v}} \quad \Delta q = \frac{2\pi}{\sqrt{S_{\text{area}}}} \quad (\text{SD}) \Rightarrow \frac{2\pi}{\sqrt{F_{\text{ov}}} \quad (\text{IF})}$$

有: $\int \frac{d^2 q dy}{(\Delta q)^2 \Delta y} \rightarrow U_{\text{bin}} \int \frac{d^2 q dy}{(2\pi)^3}$

其中: $U_{\text{bin}} = S_{\text{area}} \times \Delta \vec{v}$

若定义 $C^T = C^S + C^A + C^F$

可以得到对于一组给定的宇宙学参数 $\{\mu\}$ Fisher matrix 为

$$F_{ij}^{lm} = \frac{1}{2} U_{\text{bin}} \int \frac{dq dy}{(2\pi)^3} [\partial_i \ln C^T(q, y) \partial_j \ln C^T(q, y)]$$

也可以写成如下形式

We can rewrite (8) in terms of physical wave numbers by using the following dictionary: $V_{\text{bin}} = U_{\text{bin}} r_\nu$, $\mathbf{q} = \mathbf{k}_\perp r$, and $y = k_\parallel r_\nu$, where $k_\perp = k\sqrt{1 - \mu^2}$ and $k_\parallel = k\mu$. We then apply the substitutions

- $U_{\text{bin}} \rightarrow V_{\text{bin}}$
- $\int dq^2 dy \rightarrow 2\pi \int_{-1}^{+1} d\mu \int_{k_{\min}}^{\infty} k^2 dk$
- $q = kr\sqrt{1 - \mu^2}$ and $y = kr_\nu\mu$.

We can now express the Fisher matrix in a familiar form to those working on galaxy redshift surveys – a comparison we will pursue in Section 3.

2-4. Appendix. Fisher matrix 和相关系数

2.5. 矩阵

2.5. Experimental configurations

Our focus in this paper is on the lead-up to Phase I of the SKA. We consider a portfolio of planned experimental configurations, with the aim of exploring how they will impact constraints on cosmological parameters. Our approach is ecumenical – we try to include as many proposed configurations as possible, although we are limited by what information has been made publicly available.

We will first of all consider three illustrative experimental setups, roughly corresponding to successive ‘generations’ of planned IM experiments. These are:

- **Stage I** – Small, specialised HI experiment focused on a relatively narrow redshift range, intended to provide initial detections of the BAO and other first cosmological results. Stage I experiments are envisaged as either surveys on existing general-purpose arrays, or relatively cheap purpose-built telescopes using multi-feed receivers to improve sensitivity.
- **Stage II** – Larger interferometric experiment with enhanced sensitivity, covering a wider range of redshifts. Stage II experiments are intended to cover a substantial survey volume, with the aim of producing constraints on cosmological parameters that are competitive with contemporary (DETF³ Stage II/III) LSS surveys. They are likely to be either purpose-built HI arrays with a large number of receivers, or surveys on forthcoming ‘SKA-precursor’ arrays such as MeerKAT and ASKAP.
- **Facility** – Survey on a future large array, covering a wide redshift range over most of the sky. Facility-type surveys will compete with other large (DETF Stage IV) experiments to produce the most precise cosmological parameter estimates, and will be able to probe novel HI-only effects for the first time. The only planned experiments of this type so far are the Phase I SKA arrays, although the full CHIME and Tianlai configurations could also fall into this class.

We have chosen representative configurations for each of these classes (see Table 2) that will be used to illustrate the expected progress of HI IM experiments over the next decade. We have also forecasted for the following real (existing, proposed, or plausible) experiments:

36x12m SD

ASKAP: An SKA pathfinder consisting of thirty-six 12m dishes, each with 36-element PAFs, located at the eventual site of SKA1-SUR in Australia (Johnston et al. 2008).

BAOBAB: Proposed compact array of 128 1.6m tiles with 4 dipoles per tile, co-located with GBT or SKA1-MID (Pober et al. 2013).

BINGO: A proposed 40m (25m illuminated) multi-receiver single-dish telescope in South America (Battye et al. 2013).

CHIME: A proposed array made up of 20×100 m cylinders (20×80 m illuminated), based in British

Columbia, Canada. There is a pathfinder with 2 half-length cylinders, and a planned full experiment with 5 (CHIME Collaboration 2012).

FAST: A proposed multi-beam system on the 500m single-dish telescope currently under construction in south-west China (Smoot & Debono 2014).

GBT: A 100m single-dish telescope in West Virginia (USA). GBT has already been used for preliminary detections of the HI signal (Chang et al. 2010; Switzer et al. 2013; Masui et al. 2013).

GBT-HIM: A planned seven-beam receiver system on GBT (Chang & GBT-HIM Team 2014).

GMRT: Array of thirty 45m dishes in Pune, India (Swarup et al. 1991).

JVLA: An array of twenty-seven 25m dishes, based in New Mexico, USA (NRAO 2014).

KAT7: An SKA pathfinder made up of seven 12m dishes, on the planned site of SKA1-MID (SKA South Africa 2014).

MeerKAT: An SKA pathfinder with sixty-four 13.5m dishes, on the site of SKA1-MID (Jonas 2009). Has a choice of two frequency bands.

MFAA: A proposal for a mid-frequency aperture array component of Phase II of the SKA (MFAA 2014).

Parkes: A single 64m dish (with 13 beams) in NSW, Australia (ATNF 2014).

SKA1-MID: A planned SKA Phase I configuration with one hundred and ninety 15m dishes, based in the Northern Cape, South Africa (Dewdney et al. 2013). Can be extended to incorporate the 64 MeerKAT dishes.

SKA1-SUR: A planned SKA Phase I configuration with sixty 15m dishes, each with 36-element PAFs, based in Western Australia (Dewdney et al. 2013). Can be extended to incorporate the ASKAP dishes.

Tianlai: A proposed array of eight 15×120 m cylinders to be built in north-west China (Chen 2012).

VLBA: An array of ten 25m dishes distributed across North America (Napier et al. 1994).

WSRT + APERTIF: A proposed upgrade to WSRT that uses a phased array feed (PAF) in the focal plane to produce multiple beams on the sky (Oosterloo et al. 2010).

This is intended to be a relatively exhaustive list of current and planned HI intensity mapping experiments at $z \lesssim 3$, but inevitably some have been omitted due to a lack of publicly-available specifications. We have made our code publicly available⁴ so forecasts can be performed when specifications become available.



³See Albrecht et al. (2006).

⁴<https://gitlab.com/radio-fisher/bao21cm>

二 IM 和 3J 阶段

最有希望的 3SKA

① 小红移区域中，针对 BAO 等其他宇宙学的探测

使用现有 LF 或有 multi band receiver 的 SD

② 更大的干涉系统，具有大量的接收机和特别对 HI 阵列

和当代 LSS 调查相当的结果

	Experiments	T_{inst} [K]	$N_d \times N_b$	D_{dish} [m]	D_{\min} [m]	D_{\max} [m]	ν_{crit} [MHz]	$\nu_{\text{max}}^{\text{IM}}$ [MHz]	ν_{\min}^{IM} [MHz]	$\Delta\nu^{\text{IM}}$ [MHz]	z_{\min}	z_{\max}	S_{area} [deg 2]	
Ref.	Stage I	50	1×50	30.0	—	—	—	1100	800	300	0.29	0.77	5,000	
	• Stage II	35	160×1	4.0	4.0	53.0	1000	1000	600	400	0.42	1.37	2,000	
	Facility	20	250×1	15.0	—	—	—	1100	400	700	0.29	2.55	25,000	
Existing Facility	GBT	29	1×1	100.0	—	—	—	920	680	240	0.54	1.09	100	
	GBT-HIM	33	1×7	100.0	—	—	—	900	700	200	0.58	1.03	1,000	
	GMRT	70	30×1	45.0	—	—	—	1420	1000	420	0.00	0.42	1,000	
	JVLA	70	27×1	25.0	—	—	—	1420	1000	420	0.00	0.42	1,000	
	Parkes	23	1×13	64.0	—	—	—	1420	1155	265	0.00	0.23	5,000	
	VLBA	27	10×1	25.0	—	—	—	1420	1200	220	0.00	0.18	5,000	
	▲ WSRT + APERTIF	52	14×37	25.0	—	—	—	1300	1000	300	0.09	0.42	25,000	
Targeted IM	• BAOBAB-128	40	128×1	1.6	1.6	26.0	—	900	600	300	0.58	1.37	1,000	
	BINGO	50	1×50	25.0	—	—	—	1260	960	300	0.13	0.48	5,000	
	◊ CHIME	50	1280×1	20.0	—	—	—	800	400	400	0.77	2.55	25,000	
	FAST	20	1×20	500.0	—	—	—	1000	400	600	0.42	2.55	2,000	
	• MFAA	50	3100×1	2.4	0.1	250.0	950	950	450	500	0.49	2.16	5,000	
	◊ Tianlai	50	2048×1	15.0	—	—	—	950	550	400	0.49	1.58	25,000	
Pre-SKA	▲ ASKAP	50	36×36	12.0	—	—	—	1000	700	300	0.42	1.03	25,000	
	KAT7	30	7×1	13.5	—	—	—	1420	1200	220	0.00	0.18	2,000	
	MeerKAT (B1)	29	64×1	13.5	—	—	—	1015	580	435	0.40	1.45	25,000	
	MeerKAT (B2)	20	64×1	13.5	—	—	—	1420	900	520	0.00	0.58	25,000	
SKA Phase I	SKA1-MID (B1) Autocorr.	28	190×1	15.0	—	—	—	1050	350	700	0.35	3.06	25,000	
	◦ SKA1-MID (B1) Interferom.	28	190×1	15.0	—	—	—	1050	350	700	0.35	3.06	100	
	SKA1-MID (B2) Autocorr.	20	190×1	15.0	—	—	—	1420	900	520	0.00	0.58	25,000	
	◦ SKA1-MID (B2) Interferom.	20	190×1	15.0	—	—	—	1420	900	520	0.00	0.58	50	
	▲ SKA1-SUR (B1)	50	60×36	15.0	—	—	710	900	400	500	0.58	2.55	25,000	
	▲ SKA1-SUR (B2)	30	96×36	15.0	—	—	—	1300	1150	650	500	0.23	1.18	25,000
	SKA1-MID + MeerKAT (B1) [†]	—	—	—	—	—	—	1050	350	700	0.35	3.06	25,000	
	SKA1-MID + MeerKAT (B2) [†]	—	—	—	—	—	—	1420	900	520	0.00	0.58	25,000	

2.6. 先验信息 (Prior information)

需要加入来自其他探测器的信息，以打破 degeneracy

和提升精度。本文主要是 CMB 分布图。

CMB 数据提供高红移处的测量，有助于确定在何处用较低红移可以最有效地探测 dark energy，并提供了 matter power spectrum 的形状和 normalization。

▲
7
/ 36
▼

宇宙学参数经验采用 DETF Planck prior

$$\{h, \Omega_bh^2, \Omega_{bE}, \Omega_k, w_0, w_a, n_s, \sigma_8\}$$

GRS

3. LRG 和 Galaxy Redshift Survey 的比较
主要研究功率谱对宇宙学参数的约束. $P(k)$

⇒ 做法:

将 wavenumber 分成若干个 bin. $\Delta a = [k_a, k_{a+1}]$, 每个
 Δa 对应一个 $P_a \Rightarrow$ 预测 P_a 和误差

对于某^(GRS) experiment, S_{area} , $\bar{n}(z)$ [源的数密度]

(对于 LRG Survey: $V_{\text{bin}} = \int_{\bar{z}}^{\bar{z}'} \frac{dz}{dt} dt S_{\text{area}}$
mean redshift)

对应的 Fisher 矩阵为

$$\left\{ \begin{aligned} F_{ij}^{\text{galaxy}} &= \frac{1}{2} \int_{k_{\min}}^{k_{\max}} \frac{d^3 k}{(2\pi)^3} [\partial_i \ln P_{\text{tot}}(\vec{k}) \partial_j \ln P_{\text{tot}}(\vec{k})] V_{\text{eff}}(\vec{k}) \\ V_{\text{eff}} &= V_{\text{bin}} \left[\frac{\bar{n}(z) P_{\text{tot}}(\vec{k})}{1 + \bar{n}(z) P_{\text{tot}}(\vec{k})} \right]^2 \end{aligned} \right.$$

⇒ 只有在 $NP \gg 1$ 时功率谱方可得到很好的测量.

$$\Rightarrow \text{代入 } P_a, \text{ 得: } \langle (\frac{\delta P_a}{P_a})^2 \rangle = \left[\frac{1}{2} \int_{V_n} \frac{d^3 k}{(2\pi)^3} V_{\text{eff}}(\vec{k}) \right]^{-1}$$

而对于 IM Survey, 则有

$$\left(\frac{\Delta P_a}{P_a}\right)^2 = \left[\frac{1}{2} U_{bin} \int_{V_n} \frac{d^3 q dy}{(2\pi)^3} \left(\frac{C^s(q, y)}{C^t(q, y)} \right)^2 \right]^{-1}$$

结合我们之前已知的内参, 可以定义 V_{eff}^{IM} 和 $\bar{n}^{imp}(k) = \frac{C^s}{C^t}$.

$$\bar{n}^{IM}(z, k) = \left(\frac{T_b}{T_{sys}} \right)^2 \frac{t_{tot} \Delta v}{U_{bin}} L^{-1} B_\perp B_\parallel$$

建立了和传统 QRS 对比的桥梁

性质:

① V_{eff}^{IM} 是高度各向异性的。对于 singledish, 小于 beam 的宽度的信息都被冲掉; $k_L > D_{dish}/r_\lambda$ 的信息被压扁。
对于 interferometer, 可以看到更细微的角分辨率结构。

$$k_\perp \sim 2\pi U_{max}/r$$

② 在径向, 期望 foreground 消除所损失的信息是在 bandwidth 的尺度损失的, 即 $k_\parallel \leq k_{fg}$ 。在小尺度, 非线性速度抹掉了 $k \gtrsim 0.5 M_p c^{-1}$ 的信息。

⇒ 总结: 在大尺度上, 宇宙学变量和调查尺度为主要影响的因素。①对于 SD, 最长波长的模在径向和横向可以很好地辨别出来, $(\frac{\Delta P}{P})^2 \propto k^{-3}$

对于较小的尺度, beam size 限制了横向分辨率, $(\frac{\Delta P}{P})^2 \propto k^{-1}$

在径向, 最终会遇到 non-linear velocity scale, 抹去小于 σ_{vL} 的尺度信息。

②对于 CF, 情况和 SD 相反且互补, 由于较长的基线,

CF 可以有更高的分辨率率, $(\frac{\Delta P}{P})^2 \propto k^{-3}$, 直到达到了
 $non-linear scale$ 。超过这个极限时只有横向尺度的贡献大,
 $(\frac{\Delta P}{P})^2 \propto k^{-2}$ 直到达到了最大分辨率。

另外, CF 无法探测大于其最小基线对应的尺度。

(对应石墨子的直径, SD 模式下的 beam 大小)

二) 对于 CF 的重要特征尺度为

$$\left\{ \begin{array}{l} k_{\parallel}^{\min} \sim k_{FG} = 2\pi / (\nu_0 \Delta \tilde{\nu}_{tot}) \\ k_{\parallel}^{\max} \sim k_{NL} = 1 / \sigma_m \\ k_{\perp}^{\min} \sim k_{area} = 2\pi / \sqrt{\nu^2 S_{area}} \quad (SD) \\ \sim k_{D\min} = 2\pi D_{\min} / r_{\lambda} \quad (CF) \\ k_{\perp}^{\max} \sim k_{FOV} = 2\pi D_{dish} / r_{\lambda} \quad (SD) \\ \sim k_{D\max} = 2\pi D_{\max} / r_{\lambda} \quad (CF) \end{array} \right.$$

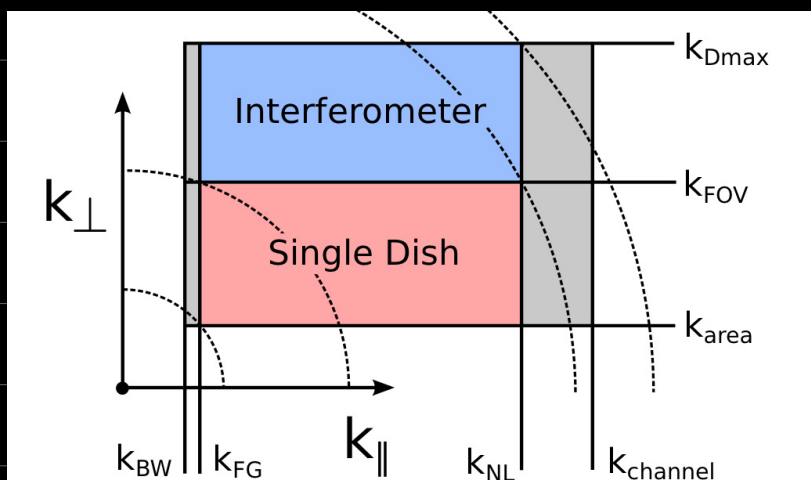


FIG. 1.— Schematic illustration of the ranges of radial and transverse wavenumbers that the two types of experiment are sensitive to. The dotted lines show the ranges in absolute wavenumber $|k|$; single-dish experiments are sensitive to smaller $|k|$ due to their lower k_{\perp}^{\min} , while interferometers can see larger $|k|$ on account of their high angular resolution. The two types of experiment are complementary in terms of their angular sensitivity, but are subject to the same constraints in frequency space.

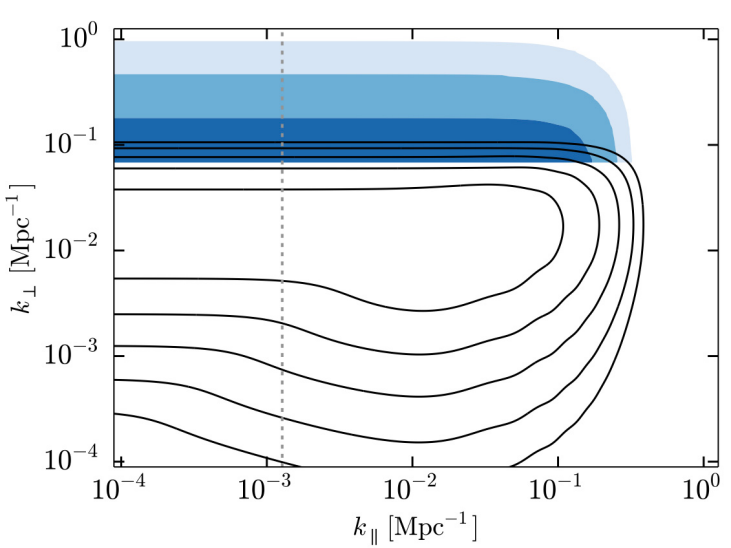


FIG. 2.— The normalised effective volume $V_{\text{eff}}(k_{\perp}, k_{\parallel})/V_{\text{bin}}$ at $z \approx 1$, for SKA1-MID Band 1 in single-dish mode (black contours) and interferometer mode (shaded blue contours). Foregrounds have not been included, but the effective minimum k_{\parallel} , given by $k_{\text{FG}} \simeq k_{\text{BW}}$, is shown as a dashed grey line. The contours are for values [0.9, 0.5, 0.1, 0.01, 0.001], where 1.0 is the maximum (implying a cosmic variance-limited measurement). Only the last three contours (i.e. < 0.5) appear for the interferometer mode due to its lower sensitivity.

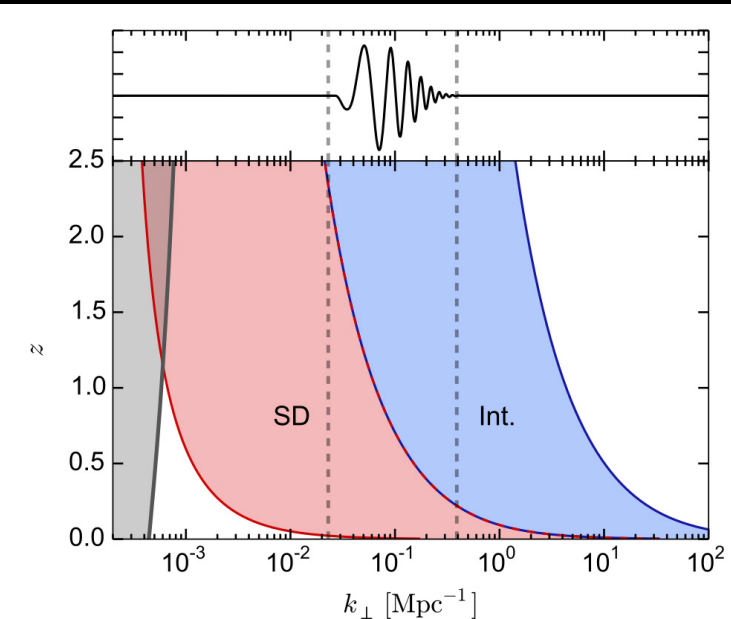


FIG. 3.— Redshift evolution of the minimum/maximum transverse scales (filled regions) for illustrative interferometer (blue) and single-dish (red) experiments. The BAO are plotted for comparison. The dishes have diameter $D_{\text{dish}} = 15\text{m}$, the min./max. interferometer baselines are $D_{\min} = 15\text{m}$ and $D_{\max} = 1000\text{m}$, and the survey has bandwidth $\Delta\nu = 600\text{ MHz}$ and area $S_{\text{area}} = 25,000\text{ sq. deg.}$. The shaded grey region denotes superhorizon scales, $k < k_H = 2\pi/r_H$.

4. (Cosmo) 打张、生长和 BAO peak

核心：测量 BAO peak 的特征尺度约束 $D_A(z)$ 和 $H(z)$
以及生长因子 $f(z)$

$$\{A(z), [b_{\text{HC}}\sigma_8](z), [\sigma_8](z), D_A(z), H(z), \sigma_8\}$$

4.1. BAO 的可探测性

关注 $P(k)$ 的误差。

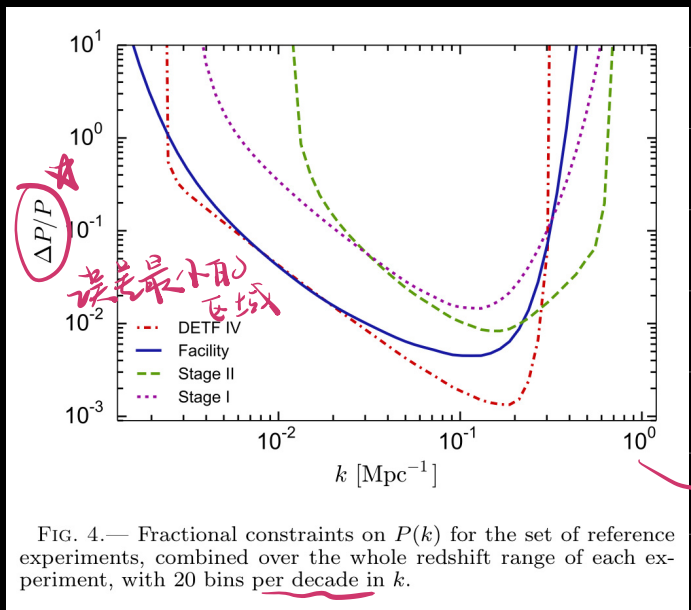


FIG. 4.— Fractional constraints on $P(k)$ for the set of reference experiments, combined over the whole redshift range of each experiment, with 20 bins per decade in k .

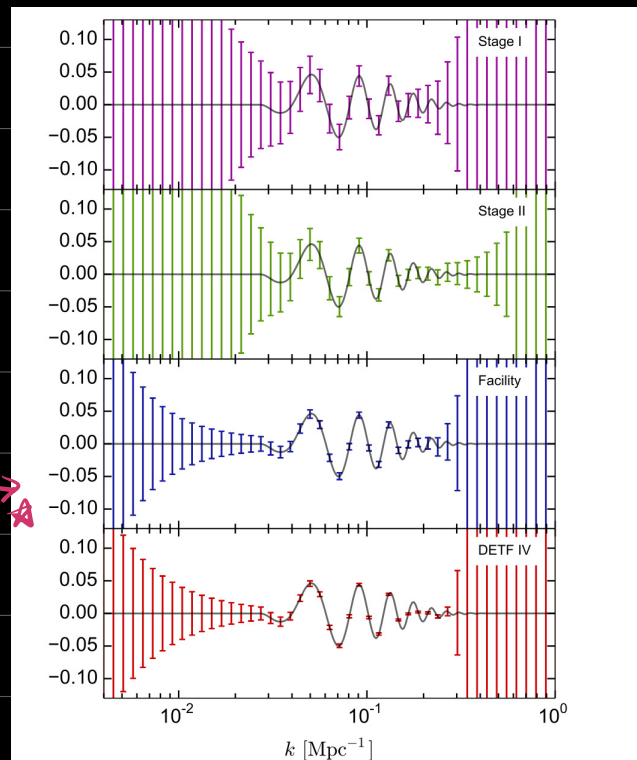


FIG. 5.— Forecast constraints on the BAO wiggles, combined over the whole redshift range for each of the reference surveys.

预期的三个阶段的约束能力

① 最终的 Facility 阶段

接近 cosmic variance limit

(由 DETF IV 阶段呈现, $k \approx 0.1 \text{ Mpc}^{-1}$)

due to the sensitivity of its SD component.

② 在 matter-radiation peak ($\sim k \sim 10^{-2} \text{ Mpc}^{-1}$) ± 10%

误差

- ③ LF 在 $k \sim 1 \text{ Mpc}^{-1}$ 指出约 10% 误差
- ④ Stage II 对小尺度结构敏感，但由于其高红移 ($z \sim 1.4$)
对 BAO 信号依然有效
- ⑤ Stage I 依然可以进行探测，但小尺度结构无法约束

对功率谱的处理

$$f_{\text{bao}}(k) = \frac{P(k) - P_{\text{smooth}}(k)}{P_{\text{smooth}}(k)}$$

引入一个 amplitude 参数

$$P(k) = [1 + A f_{\text{bao}}(k)] P_{\text{smooth}}(k)$$

\Rightarrow Construct a "purely oscillatory" $f_{\text{bao}}(k)$

① 用 CAMP 包计算 $P(k)$ ，选出振荡最显著的

区域，用三次样条拟合 $\ln P(k) \sim \ln(k)$

② 构建初步的振荡函数 $P(k)/P_{\text{spine}}(k)$ ，再以二次

cubic spline 插值，找到二阶导零点（中点）

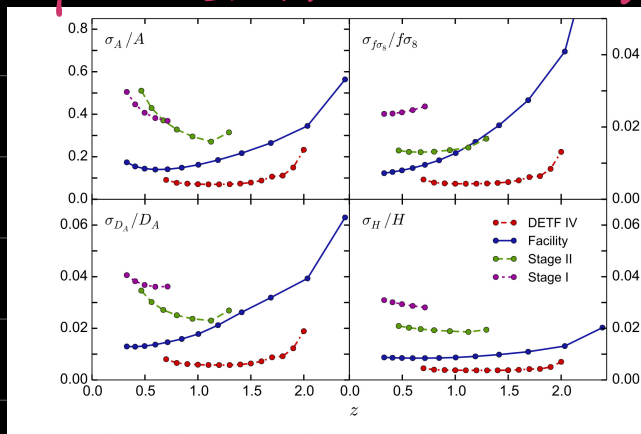


FIG. 6.— Fractional errors on $A(z)$, $f\sigma_8(z)$, $D_A(z)$, and $H(z)$, as a function of redshift.

4.2. 对 $D_A(z)$ 和 $H(z)$ 的约束

$D_A(z)$: 角直径距离

$H(z)$: expansion rate.

输入:

$$\alpha_L = \frac{r^{\text{fid}}}{r} = \frac{D_A^{\text{fid}}(z)}{D_A(z)}$$

$$\alpha_{\Lambda} = \frac{r_{\Lambda}}{r} = \frac{H(z)}{H^{\text{fid}}(z)}$$

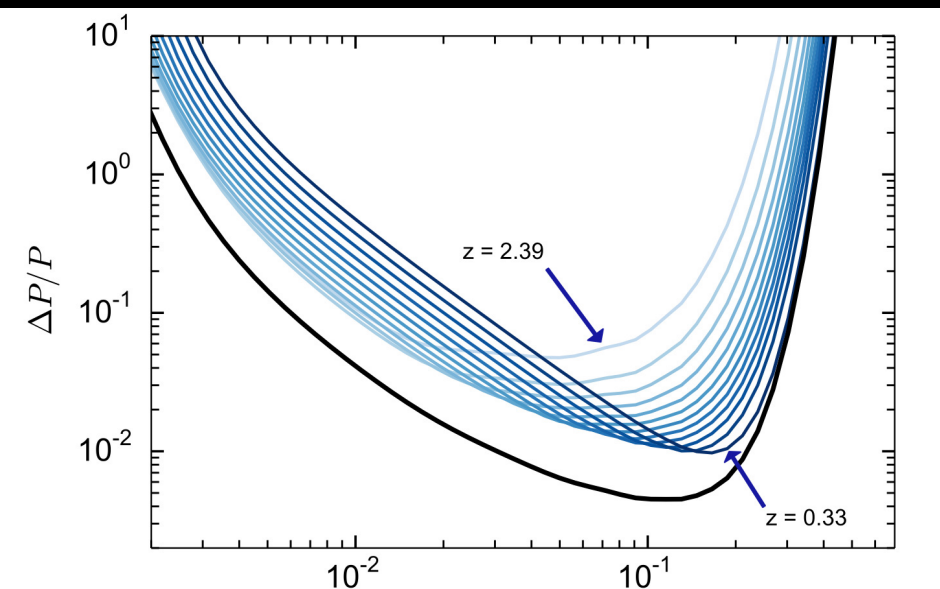
fiducial
 Λ CDM
values

导致 $P(k)$ 的各向同性
 \rightarrow 并测量距离

则得到. ($q \rightarrow \alpha_L q$ $y \rightarrow \alpha_{\Lambda} y$) Alcock-Paczynski effect

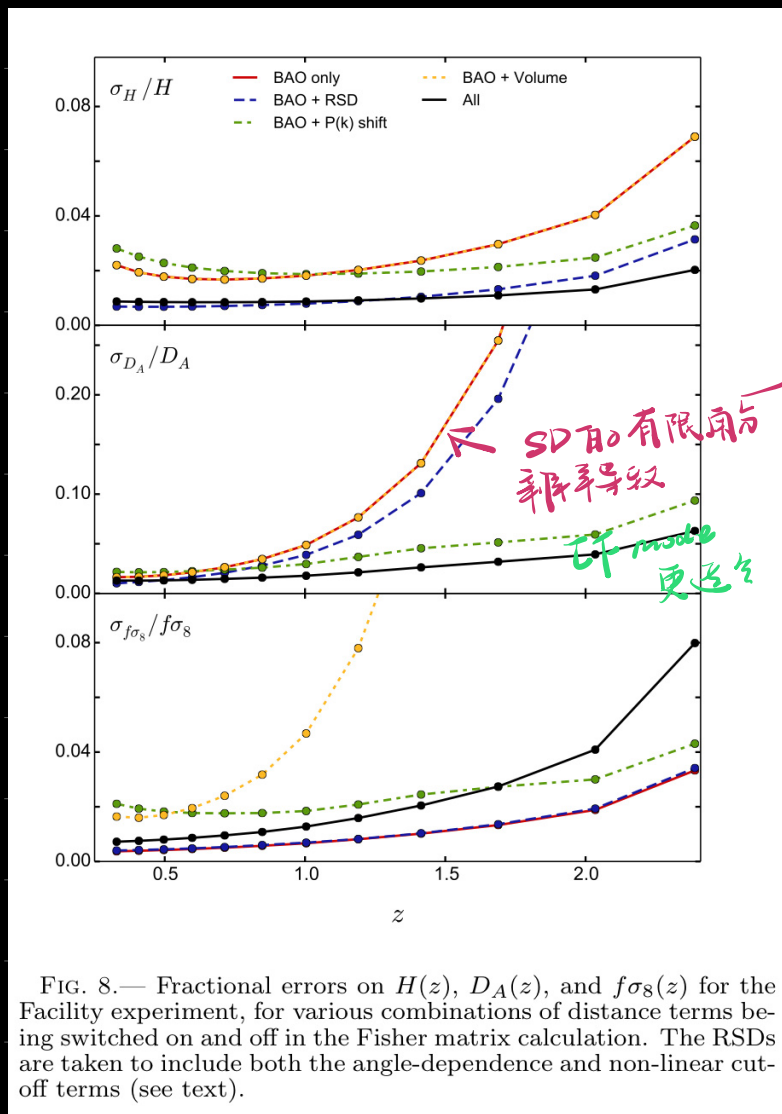
$$C^S(q, y) = T_b^2 \frac{\alpha_L^2 \alpha_{\Lambda}}{r^2 r_{\Lambda}} F_{RSD} \left(\frac{\alpha_L q}{r}, \frac{\alpha_{\Lambda} y}{r} \right) D(z) \times P(k = \sqrt{\left(\frac{\alpha_L q}{r} \right)^2 + \left(\frac{\alpha_{\Lambda} y}{r} \right)^2}) RSD_s$$

由于系统误差的 Robust, BAO 是测距的首选.



不同红移下 不同 k [Mpc $^{-1}$]
bin 的大小对 $\Delta P/P$ 的限制能力

FIG. 7.— Fractional constraints on $P(k)$ in each redshift bin, for the Facility experiment. The thick black line is the total constraint, summed over all redshift bins.



在不同红移段
对宇宙学参数的约束能力
忽略某些效应后才
测量精度的提升

FIG. 8.— Fractional errors on $H(z)$, $D_A(z)$, and $f\sigma_8(z)$ for the Facility experiment, for various combinations of distance terms being switched on and off in the Fisher matrix calculation. The RSDs are taken to include both the angle-dependence and non-linear cut-off terms (see text).

需要注意的是，若BAO只用于测距离 $D_A(z)$ 和 $H(z)$ 会受到横向与非线性的影响。

研究一个模拟模型。

$$v_{BAO}(r) = A \exp\left(-\frac{(r - r_{BAO})^2}{2\sigma^2}\right)$$

对沿横向的分辨率损失的反应相当于将相关函数
和窗口函数进行卷积。

5. 宇宙学参数

通过线性映射将旧参数集映射到新参数集，即

$$F(\beta) = \sum_i M_i^T F_i(\alpha) M_i$$

其中 $\alpha = \{f(z), D_A(z), H(z)\}$

$$\beta = \{h, \Omega_{DE}, \Omega_K, w_0, w_a, \sigma_8\}$$

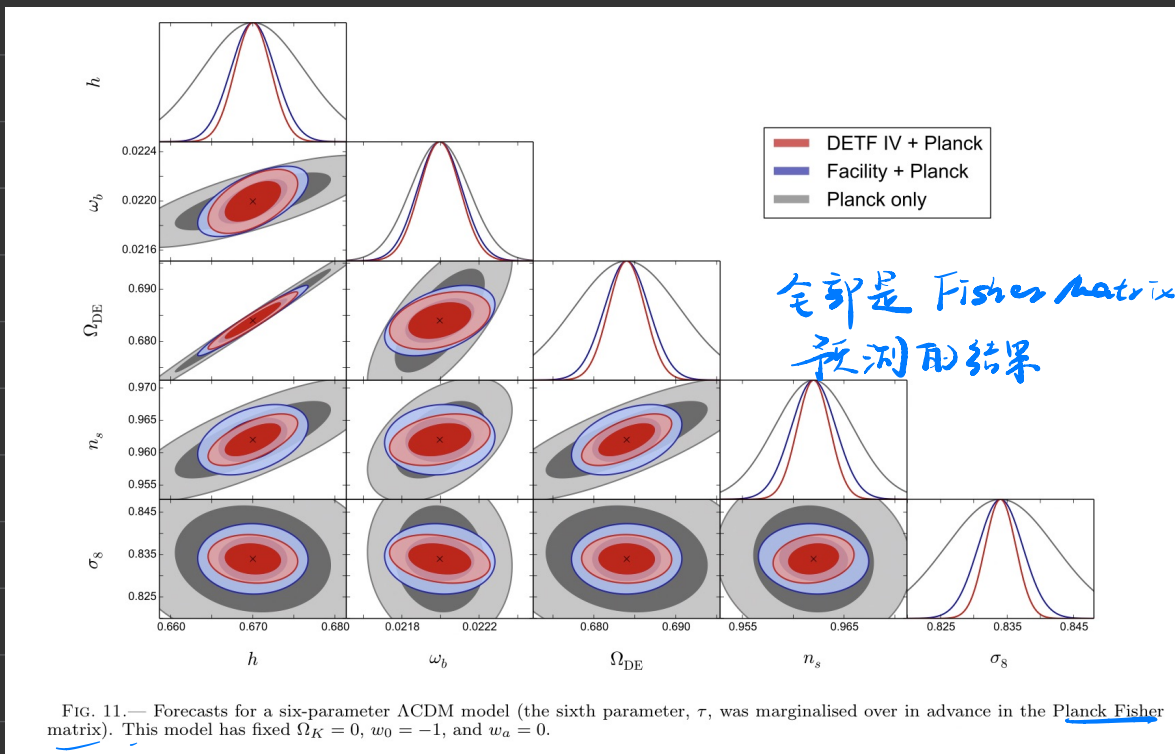
\Rightarrow 其中也含有 $\{n_s, \sigma_8\}$ 的信息。…… \downarrow full set

$$\beta = \{h, \Omega_{DE}, \Omega_K, w_0, w_a, n_s, \sigma_8, \tau, A(z), b_{HI}(z), \sigma_m, w_b\}$$

w_b : baryon density. $w_b = S_b h^2$, 不由 HI experiments 得出, 而是含于 Planck prior 之中。

total matter density $\Omega_M = 1 - \Omega_K - \Omega_{DE}$

\Rightarrow 利用 LIGO 和 Planck CMB data 结合对 Λ CDM model 的预测



11m.

Experiments	h $/10^{-3}$	ω_b $/10^{-4}$	Ω_{DE} $/10^{-3}$	n_s $/10^{-4}$	σ_8 $/10^{-3}$
Planck + Stage I	5.8	1.5	6.1	36.9	7.0
Planck + Stage II	5.1	1.4	5.3	32.8	6.0
Planck + Facility	2.7	1.2	2.7	21.9	3.3
Planck + DETF IV	2.2	1.0	2.2	16.0	2.3
Planck + WMAP	12	2.8	17	73.0	12
Planck+WP+BAO	7.8	2.5	10	57.0	11

TABLE 3
FORECAST 1σ MARGINAL ERRORS ON VANILLA Λ CDM MODEL
PARAMETERS FOR THE SET OF REFERENCE SURVEYS, COMPARED
WITH CURRENT CONSTRAINTS FROM PLANCK (TEMPERATURE-ONLY)
AND WMAP (PLANCK COLLABORATION 2013B).

加入 LSS Data 的最大效果是提高了 h 和 σ_8 的约束

由于 SD 的角分辨率限制, LSS 不好约束和 $k \sim 0.1 \text{ Mpc}^{-1}$ 相关的参数

5.2. 暗物质状态方程

$$w(a) = w_0 + \frac{z}{1+z} w_a$$

(

$$\Omega_{\text{DE}}(z) = \Omega_{\text{DE},0} \exp[\beta w_0 z / (1+z)] (1+z)^{3(1+w_0+w_a)}$$

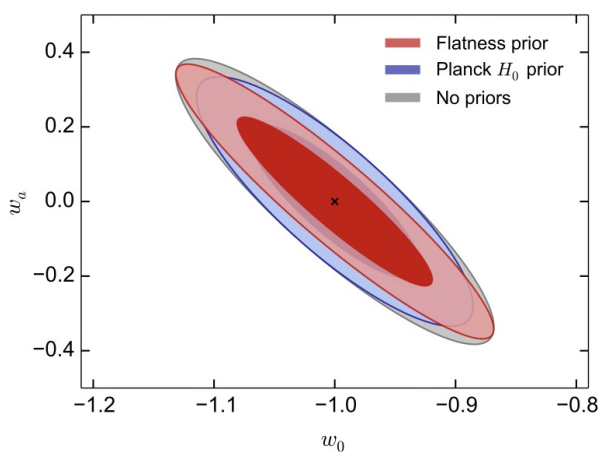


FIG. 12.— Effect of various priors on $w_0 - w_a$ constraints, for Facility + Planck. Ω_K is already well-constrained by the combination of CMB and HI data, so the flatness prior has only a small effect. Additional H_0 information has a larger effect in breaking the degeneracy.

Energy Task Force as (Albrecht et al. 2009)

$$\text{FOM} = 1/\sqrt{\det(F^{-1}|_{w_0, w_a})}, \quad (23)$$

which is proportional to the reciprocal of the area enclosed by the 68% contour of the (w_0, w_a) error ellipse for Fisher matrix F .

The foremost task in understanding the nature of dark energy is to determine whether the equation of state dif-

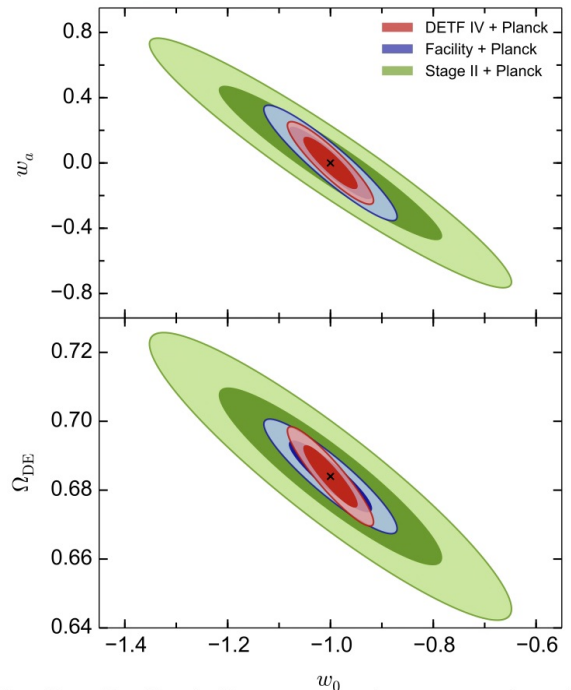


FIG. 13.— Top Panel: Forecast constraints on w_0 and w_a , including the Planck prior. We have assumed flatness ($\Omega_K = 0$), and fixed γ to its fiducial value. The DETF figures of merit for the Stage II, Facility, and DETF Stage IV surveys are 95, 358 and 712 respectively. Bottom Panel: Forecast constraints on w_0 and Ω_{DE} for the same setup.

Experiments	A /10 ⁻²	h /10 ⁻³	Ω_K /10 ⁻⁴	Ω_{DE} /10 ⁻³	n_s /10 ⁻⁴	σ_8 /10 ⁻³	γ /10 ⁻²	w_0 /10 ⁻²	w_a /10 ⁻²	FOM
Stage I	18.9	32.3	47.9	22.3	38.5	8.1	3.6	31.3	85.2	13.8
Stage II	13.2	23.7	33.1	17.2	38.0	7.8	4.4	15.2	33.1	39.9
Facility	5.2	8.7	13.6	6.9	35.0	6.0	1.8	5.4	14.9	265.4
GBT	73.9	131.9	178.4	93.4	38.6	8.2	20.1	95.0	221.8	1.1
GBT-HIM	31.2	64.3	78.9	45.4	38.6	8.2	9.8	50.7	126.9	4.2
GMRT	54.3	37.1	153.0	19.3	38.5	8.2	4.1	35.8	184.2	7.0
JVLA	57.7	43.0	175.3	22.6	38.6	8.2	4.5	40.1	209.2	5.5
Parkes	51.2	28.4	322.6	32.6	38.4	8.2	2.7	44.7	335.5	3.6
VLBA	74.8	47.8	826.9	86.2	38.6	8.2	3.8	91.7	799.8	0.8
WSRT + APERTIF	11.2	11.1	41.2	6.5	37.7	8.0	1.5	15.1	66.4	57.6
BAOBAB-128	24.3	50.2	71.3	36.6	38.5	8.1	9.0	33.3	71.4	8.0
BINGO	25.8	30.8	90.0	16.1	38.5	8.2	2.8	44.1	172.5	7.8
CHIME	3.0	8.7	9.7	7.1	30.2	5.2	3.4	5.0	15.1	288.1
FAST	7.5	13.5	16.0	10.1	33.5	6.4	3.2	7.1	18.5	144.7
MFAA	5.7	11.9	14.1	9.1	32.2	6.0	3.1	6.3	17.2	165.7
Tianlai	3.6	8.0	11.9	6.3	28.7	4.9	2.4	4.0	12.0	383.3
ASKAP	7.7	16.2	21.1	11.9	37.8	7.7	2.9	11.8	26.8	80.3
KAT7	114.0	76.4	1182.5	124.1	38.6	8.2	5.8	130.1	1138.6	0.4
MeerKAT (B1)	12.2	24.4	29.4	17.9	38.1	7.9	3.6	17.4	38.4	35.9
MeerKAT (B2)	10.2	9.4	26.8	6.1	37.5	7.7	1.5	6.4	29.5	171.4
SKA1-MID (B1) Autocorr.	6.2	11.2	16.1	8.7	35.9	6.6	2.3	7.1	17.6	162.5
SKA1-MID (B1) Interferom.	22.3	29.1	34.3	19.9	37.2	7.8	8.7	13.6	33.8	45.1
SKA1-MID (B2) Autocorr.	7.6	7.1	18.6	5.1	35.9	7.2	1.3	3.6	16.4	410.9
SKA1-MID (B2) Interferom.	368.2	37.3	94.3	19.0	38.0	8.2	10.6	22.8	86.5	18.5
SKA1-SUR (B1)	5.3	11.9	15.2	9.3	35.4	6.7	3.3	6.5	16.0	159.5
SKA1-SUR (B2)	4.5	6.5	12.2	5.3	35.3	5.7	1.4	3.8	12.2	444.2
SKA1-MID + MeerKAT (B1)	6.4	11.6	16.7	9.0	36.1	6.8	2.4	7.5	18.2	148.9
SKA1-MID + MeerKAT (B2)	7.7	7.1	18.6	5.1	35.9	7.2	1.3	3.5	16.3	414.7
DETF Stage IV (gal. survey)	2.4	7.5	8.6	6.2	27.1	5.3	3.2	4.1	12.8	405.5
Fiducial values	1.0	0.67	0.0	0.684	0.962	0.834	0.55	-1.0	0.0	-

TABLE 4

1D MARGINAL CONSTRAINTS (68% CL) ON THE EXTENDED Λ CDM MODEL, INCLUDING THE PLANCK PRIOR. THE CONSTRAINT ON A (WHICH HAS BEEN SUMMED OVER ALL REDSHIFT BINS) GIVES A MEASURE OF THE DETECTABILITY OF THE BAO.

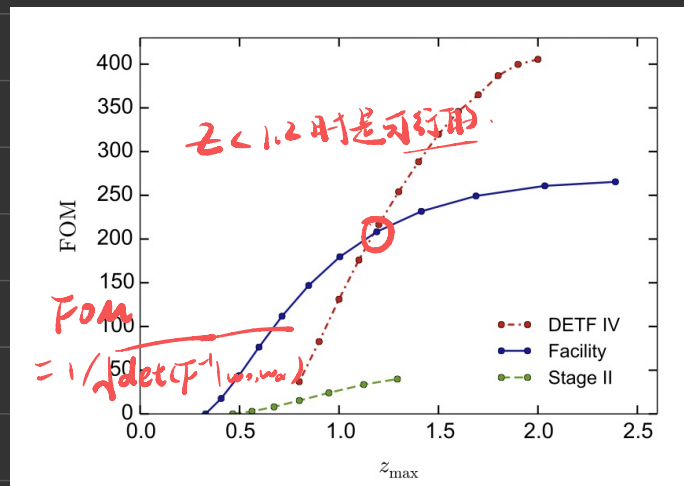


FIG. 14.— Improvement in dark energy FOM as a function of the maximum redshift of the survey (Ω_K and γ marginalised).

5.3. Curvature

可探测的曲率精度大概在 10^{-4} 对参数的半误差

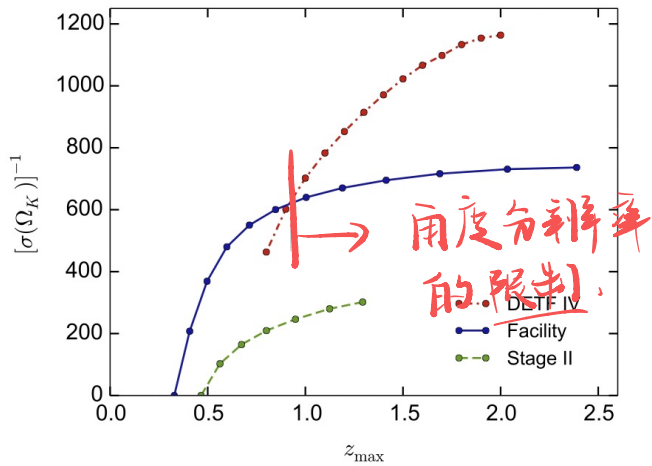


FIG. 15.— Improvement in Ω_K constraints as a function of maximum redshift of the survey. We have marginalised over w_0 , w_a and γ here.

inflating models would be put under pressure (Kleban &
 Geshi 2012; Cai et al. 2012)

对膨胀晚期的认识的改进最有助于分离曲率和暗能量的影响。

(Fig 15)

5.4. Parametrised growth survey

宇宙的演化历史是对GR理论的有力检验，但是修正引力的特征和其他天体物理效应产生混合。 \Rightarrow 线性速度场为最可能观测到的效应。

Peebles 的最简单的参数化

$$f(z) = S_m^y(z)$$

Λ CDM+GR: $f_{\text{GR}} \approx 0.5$

Caution:

① γ 并非为常数, $\gamma(z)$

② 不用修改GR 和 DM/DE 模型也可以修改增长历史 $f(\omega)$

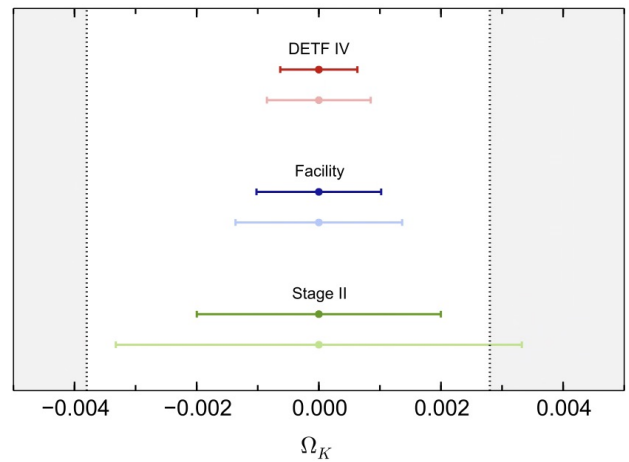
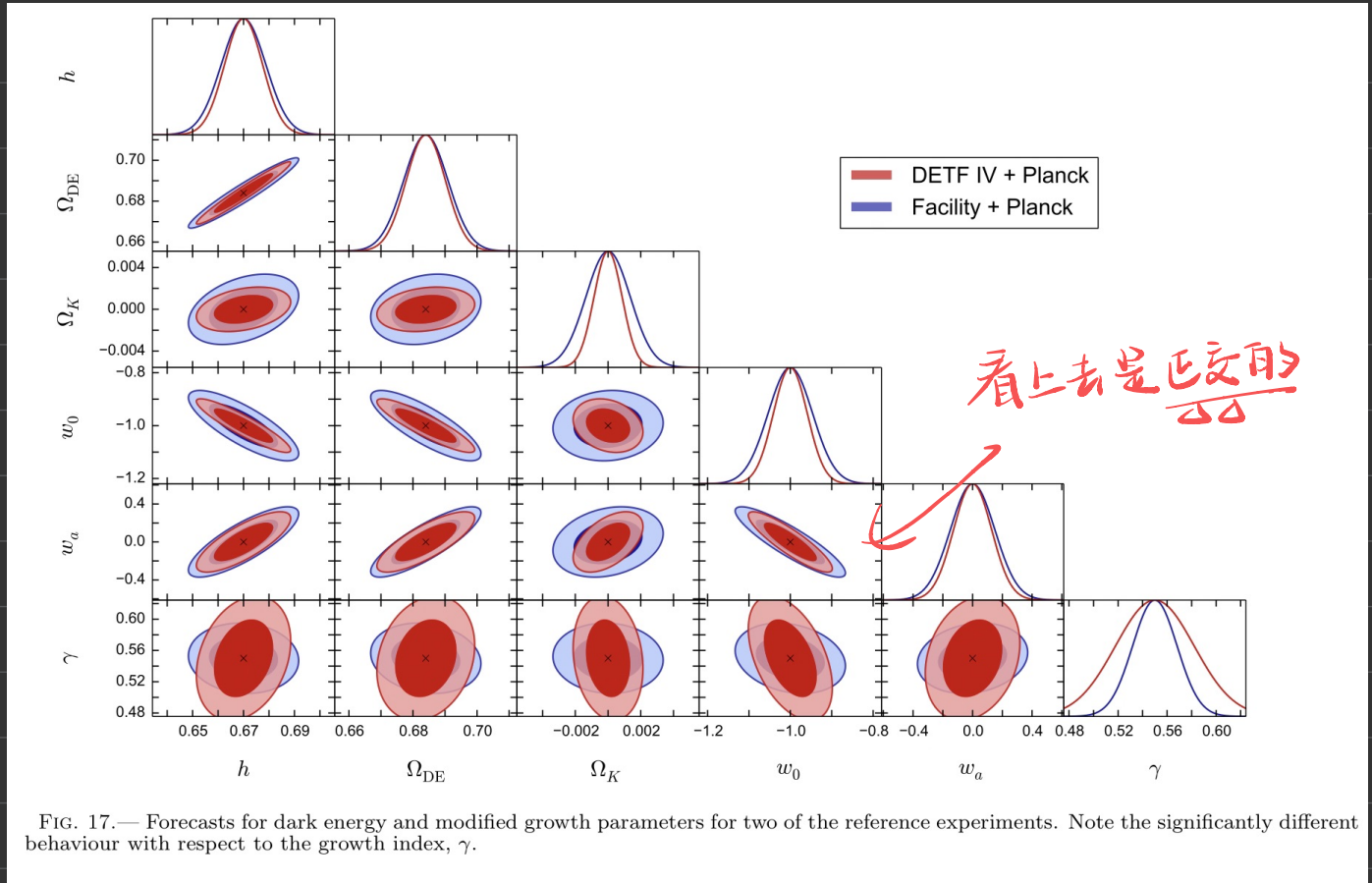


FIG. 16.— Forecast marginal constraints on Ω_K (68% CL) for the reference experiments plus Planck, with (w_0, w_a) fixed to their fiducial values (upper errorbars), and marginalised over (lower errorbars). The shaded area shows the current best constraint on Ω_K (w_0, w_a fixed) from Planck + WMAP + high- ℓ CMB + BAO (Planck Collaboration 2013b).



6. Systematic effects

IM 有自身的系统性问题

6.1. Cosmo HI signal 的演化

fiducial value. $\sigma_{\text{HI},0} = 6.5 \times 10^{-4}$

和我们的实验最相关的是 WiggleZ galaxy redshift survey.

At $z=0.8$,

$$\sigma_{\text{HI}} b_{\text{HI}} \bar{\nu} \sim [4.3 \pm 0.7 \text{ (stat.)} \pm 0.4 \text{ (sys.)}] \times 10^{-4}$$

$\bar{\nu} \approx 0.9 \sim 0.95$, $0.075 h \text{ Mpc}^{-1} < k < 0.3 h \text{ Mpc}^{-1}$
关联系数

若拓展到 $0.04 h \text{ Mpc}^{-1} < k < 0.8 h \text{ Mpc}^{-1}$

$$\Omega_{\text{HI}} b_{\text{HI}} \bar{\tau} = [4.0 \pm 0.5 (\text{stat.}) \pm 0.4 (\text{sys.})] \times 10^{-4}$$

数值模拟发现, $b_{\text{HI}} \sim 0.55 - 0.66$

⇒ 不同方法得到的结果是：

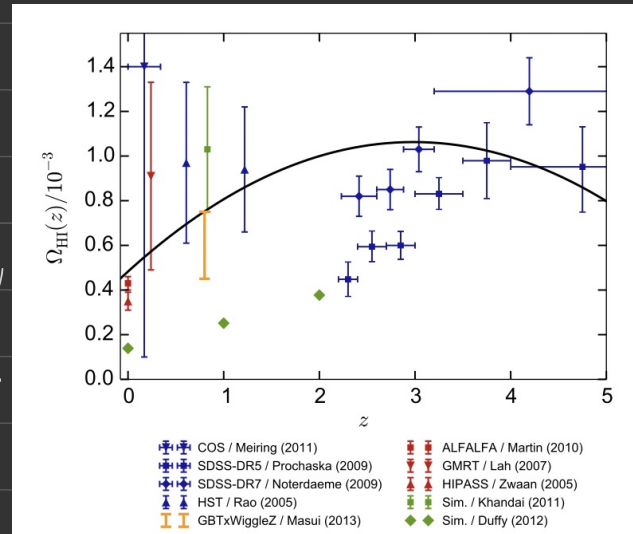


FIG. 20.— Current constraints on the HI density fraction as a function of redshift, $\Omega_{\text{HI}}(z)$ (Meiring et al. 2011; Prochaska & Wolfe 2009; Noterdaeme et al. 2009; Rao et al. 2006; Martin et al. 2010; Lah et al. 2007; Zwaan et al. 2005; Khandai et al. 2011), partially based on the compilation in Duffy et al. (2012) (see also Padmanabhan et al. 2014). DLA observations are shown in blue, cross-correlations in yellow, other observations in red, and simulations in green. The thick black line shows the fiducial $\Omega_{\text{HI}}(z)$ that we have adopted in this paper, which has $\Omega_{\text{HI}}(z=0) = 4.86 \times 10^{-4}$.

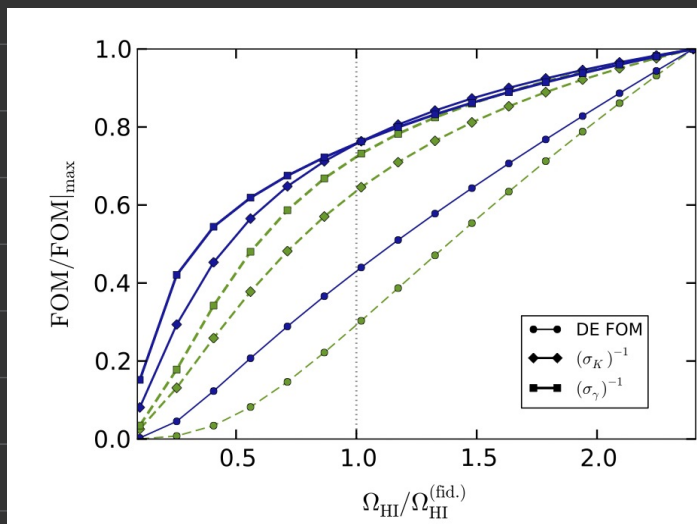


FIG. 21.— Normalised FOM and Ω_K and γ marginal errors, as a function of Ω_{HI} rescaled by a constant factor, for the Facility (blue, solid) and Stage II (green, dashed) surveys.

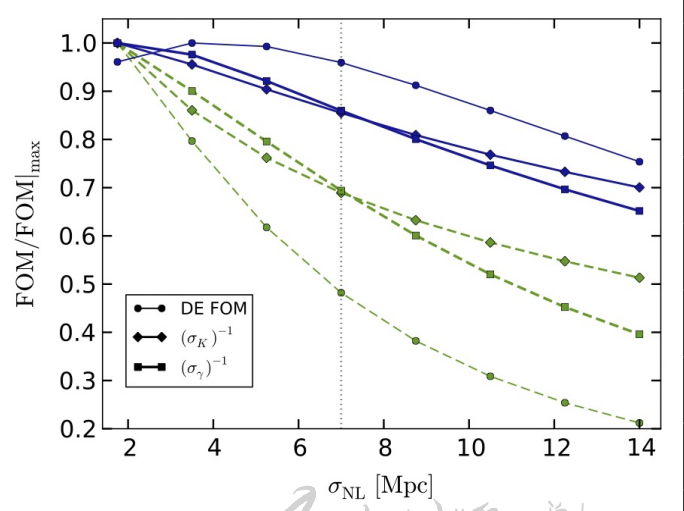


FIG. 22.— Normalised FOM/marginal errors as a function of σ_{NL} (see Fig. 21 for key).

用一个恒定的因子重新缩放
HL 对几个观测指标的影响

6.3. 前景

问题：对前景加权系数理解也不了解。

无法干净地干掉前景 ② 用残余噪声泛模拟前景的影响

(Sec 2.3, ϵ_{FG} , k_{FG} : minimum cutoff wavenumber.)

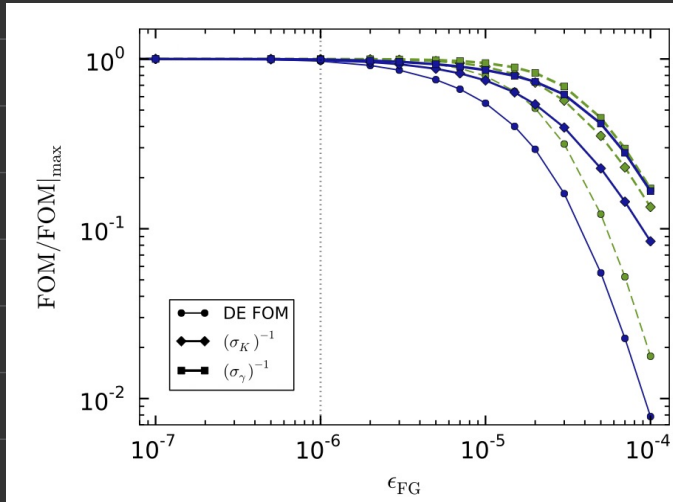


FIG. 23.— Normalised FOM/marginal errors as a function of ϵ_{FG} (see Fig. 21 for key).

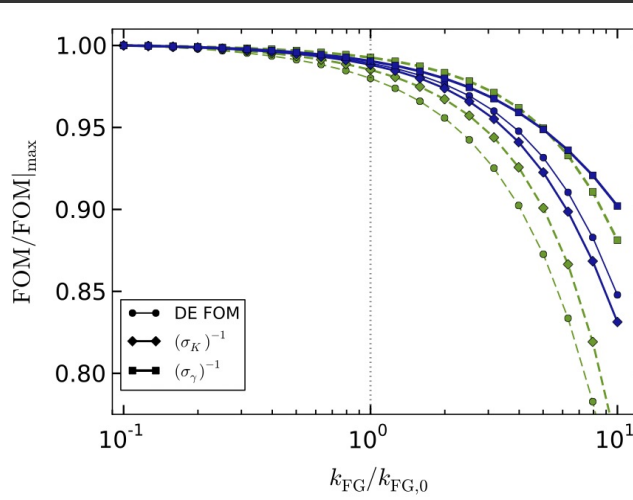


FIG. 24.— The effect of rescaling the foreground cutoff scale, k_{FG} , on the normalised FOM/marginal errors (see Fig. 21 for key). The base value of the cut-off scale is $k_{\text{FG},0} = 2\pi/(r_\nu \Delta\nu_{\text{tot}})$.

极化前景和非极化前景会产生交叉影响

同步辐射 - Faraday 无线电。

$$\phi(r) = \phi_0(r) + C r^{-2} \int_0^r n e(r') \vec{B}(r') dr'$$

\Rightarrow 通过加大 ϵ_{FG} 解决

6.4、自相关性校准 (SD)